

Joint Identifiability of Cross-Domain Recommendation via Hierarchical Subspace Disentanglement

Jing Du^{*†}
Macquarie University
Sydney, Australia
jing.du@mq.edu.au

Zesheng Ye^{*}
The University of New South Wales
Sydney, Australia
zesheng.ye@unsw.edu.au

Bin Guo
Northwestern Polytechnical
University, China
guobin.keio@gmail.com

Zhiwen Yu
Northwestern Polytechnical
University, China
zhiweny@gmail.com

Lina Yao[‡]
CSIRO's Data 61
Sydney, Australia
lina.yao@unsw.edu.au

ABSTRACT

Cross-Domain Recommendation (CDR) seeks to enable effective knowledge transfer across domains. Most existing works rely on either representation alignment or transformation bridges, but they come with shortcomings regarding *identifiability* of domain-shared and domain-specific latent factors. Specifically, while CDR describes user representations as a joint distribution over two domains, these methods fail to account for its *joint identifiability* as they primarily fixate on the marginal distribution within a particular domain. Such a failure may overlook the conditionality between two domains and how it contributes to latent factor disentanglement, leading to negative transfer when domains are weakly correlated. In this study, we explore what *should* and *should not be transferred* in cross-domain user representations from a causality perspective. We propose a **Hierarchical** subspace disentanglement approach to explore the **Joint IDentifiability** of cross-domain joint distribution, termed **HJID**, to preserve domain-specific behaviors from domain-shared factors. HJID abides by the feature hierarchy and divides user representations into generic shallow subspace and domain-oriented deep subspaces. We first encode the generic pattern in the shallow subspace by minimizing the Maximum Mean Discrepancy of initial layer activation. Then, to dissect how domain-oriented latent factors are encoded in deeper layers activation, we construct a cross-domain causality-based data generation graph, which identifies cross-domain consistent and domain-specific components, adhering to the Minimal Change principle. This allows HJID to maintain stability whilst discovering unique factors for different domains, all within a generative framework of invertible transformations that guarantee the *joint identifiability*. With experiments on

real-world datasets, we show that HJID outperforms SOTA methods on a range of strongly and weakly correlated CDR tasks.

KEYWORDS

Cross-Domain Recommendation, Subspace disentanglement, Identifiable joint distribution

ACM Reference Format:

Jing Du, Zesheng Ye, Bin Guo, Zhiwen Yu, and Lina Yao. 2024. Joint Identifiability of Cross-Domain Recommendation via Hierarchical Subspace Disentanglement. In *Proceedings of ACM Conference (Conference'17)*. ACM, New York, NY, USA, 11 pages. <https://doi.org/10.1145/nmnnnnn.nmnnnnn>

1 INTRODUCTION

Cross-Domain Recommendation (CDR) leverages information from the source domain to the target domain to achieve robust predictions in both domains [6, 23]. Let U_x and U_y denote user representations for the source domain and the target domain, each associated with a domain identifier $\{X, Y\}$. A probabilistic viewpoint interprets CDR methods by modeling a joint distribution $P(U_x, U_y)$ with a representation generator capable of optimally inferring user representations U_y in the target domain, using observed source user representations U_x , and vice versa. From this joint distribution, it becomes feasible to deduce marginal distributions describing user behaviors for each domain, specifically $P(U_x)$ and $P(U_y)$.

With this formulation, we can partition previous CDR studies into three pivotal categories, as shown in Fig. 1: **Alignment method**, **Bridge method**, and **Constraint method**. The **Alignment method**, featured in [40, 44, 47], employs either explicit sharing or implicit alignment of users feature spaces across domains. These methods enforce $P(U_x) = P(U_y)$, thus facilitating the consistency of user representations in both domains. The **Bridge method** assumes a user's representation can be transferred from one source to another via bespoke neural architectures [22, 35, 55], which craft a function $\phi(\cdot)$ to map the marginal distribution from one to another $P(U_y) = \phi(P(U_x))$. These methods, however, consider user representation as a whole and are fully transferable, potentially leading to negative transfer if improper transformations are applied to non-transferable components [54]. To address this, recent studies have veered towards **Constraints method** [9, 10, 13]. These studies emphasize identifying domain-shared components from user representations, and constraining their consistency across domains.

^{*}Jing Du and Zesheng Ye share equal contributions as co-first authors.

[†]Work done during Jing Du's studies at the University of New South Wales.

[‡]Lina Yao is also affiliated with the University of New South Wales and Macquarie University.

Permission to make digital or hard copies of all or part of this work for personal or classroom use is granted without fee provided that copies are not made or distributed for profit or commercial advantage and that copies bear this notice and the full citation on the first page. Copyrights for components of this work owned by others than ACM must be honored. Abstracting with credit is permitted. To copy otherwise, or republish, to post on servers or to redistribute to lists, requires prior specific permission and/or a fee. Request permissions from permissions@acm.org.

Conference'17, July 2017, Washington, DC, USA

© 2024 Association for Computing Machinery.

ACM ISBN 978-x-xxxx-xxxx-x/YY/MM...\$15.00

<https://doi.org/10.1145/nmnnnnn.nmnnnnn>

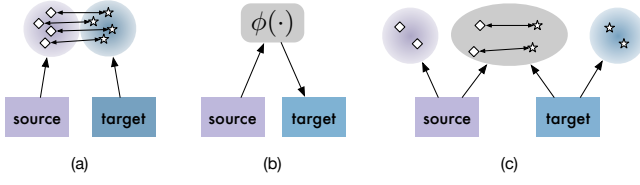


Figure 1: (a) Alignment method; (b) Bridge method; (c) Constraint method.

Nevertheless, even **Constraints** methods tend to focus overwhelmingly on extracting domain-shared, transferable features [9, 10, 31], implicitly assuming the remaining, i.e., domain-specific representations are mutually exclusive for different domains. That is, the domain-specific latent factors for X have no influence on the user behavior in Y , and vice versa. However, from a user preference viewpoint, U_x and U_y inherently suggest the user’s intrinsic preference shifts to different domains X and Y , but not necessarily imply they are independent quantities [41], otherwise it might be overly restrictive. To illustrate, we assume U is a Gaussian random variable in the simplest case, whose mean can be viewed as domain-shared factors arise from behavioral consistency, whereas domain-specific factors deliver observation variances owing to distribution shifts across domains¹. The correlation between domain-specific factors should be captured, even when they are approximated within disparate domains. Moreover, the marginal distributions $p(U_x)$ and $p(U_y)$, due to coming from the same user [9, 19], should match a unique joint distribution, namely *joint identifiability*. None of the previous methods, however, are tailored to confirm the identifiability of $P(X, Y)$, rendering them unable to uniquely recover latent factors and vulnerable to distribution shifts between domains [11, 43].

Accordingly, we propose to model a cross-domain user representation that uniquely derives the *joint identifiability* of $p(U_x, U_y)$. This allows us to disentangle the user representation into a shared portion for cross-domain consistent behavioral preference, and an adaptable portion for domain-specific patterns [19, 42, 50], leading to improved model generalization and interpretability. Specifically, we incorporate two fundamental principles: *Feature Hierarchy* (FH) [48] of Deep Neural Network and *Minimal Change* (MC) [5, 36] of Causal Inference as the cornerstones. Using a Dual-stream Deep Adaptation Network-like architecture [33], we follow the FH principle that encodes general, less domain-oriented features from the user-item interactions in respective domain with initial (shallow) layers, whereas capturing more domain-oriented features within deeper layers [29]. The FH principle not only bridges the distributional discrepancy between domains, but also leaves exploration of domain-specific information to the deeper level feature space. Furthermore, the MC principle [24, 25] praises the minimal alterations to an existing model during inference to mitigate interference. Leveraging the MC principle and the causal relationships in user representations, we attempt to characterize the domain shifts between X and Y with U_x and U_y . Recall that we have considered deeper-level network activation as a comprehensive description of user preference that preserves consistency (through a shared, cross-domain stable facet) and highlights specificity (through the

adaptable, cross-domain variant facet). In line with the MC principle, we attribute the domain shifts, signified by divergences in U_x, U_y , to this variant facet, provided that *joint identifiability* enables the disentanglement of user representation.

More concretely, we introduce **HJID** for CDR targeting the goals outlined above. Using the FH principle, we first divide the user representation into shallow and deeper subspaces corresponding to neural network layers. Within the shallow network layers, we align the activations (representations) between source and target domains with Maximum Mean Discrepancy to achieve cross-domain consistency in general features. Following, we formulate a data generation graph for deep-level representation to depict the distribution shifts within CDR. In this graph, we disentangle deeper layer representations into cross-domain stable and variant latent factors, defining their causal relationship using a latent variable generative model. According to the MC principle, the stable portion remains consistent across domains, ensuring the continuity of intrinsic user preference. On the other hand, we enforce the variant part to model cross-domain user variances under tractable and invertible transformations. We implement a generative Flow model [12] to map the domain-specific factors between the source and the target domain, which characterizes how these factors in one domain relate to user behaviors in another. This allows us to reduce the impact of distribution shifts while ensuring identifiability of the joint distribution over cross-domain user representations. Notably, our approach focuses on modeling the distributional trends with randomly sampled groups of users, sidestepping the need for exact overlap of user behaviors in two domains. That is, it is universally applicable to CDR tasks, irrespective of whether users overlap.

The contributions of our work are summarized as follows:

- For overall motivation, we present **HJID**, a hierarchical, generative, and causal discovery-driven approach for *identifiable* joint distribution of cross-domain user representation, through disentangling user representation into cross-domain stable and variant components. Namely, **HJID** highlights *joint identifiability* in CDR, enabling unique latent factor recovery with limited user-item interactions and thus improved robustness under uncertain CDR scenarios.
- For disentanglement, we formulate a causal data generation graph to identify cross-domain stable facet from variant facet, referred to as domain-shared and domain-specific latent factors.
- For domain shift, we challenge the previous assumption on mutually exclusive domain-specific factors, instead learning to capture their correlations with invertible transformations, ensuring *joint identifiability* under distribution shift.

2 PRELIMINARIES

Let $\{X, Y\}$ be two recommendation domains. In domain X , we have a user set $\mathbb{U}_x = \{u_i\}^{|\mathbb{U}_x|}$ and an item set $\mathbb{V}_x = \{v_j\}^{|\mathbb{V}_x|}$. The interaction set $\mathbb{E}_x = \langle u_i, v_j \rangle, \forall u_i \in \mathbb{U}_x, \forall v_j \in \mathbb{V}_x$ with $\langle u_i, v_j \rangle = 1$ indicating user i has interacted with item j , else $\langle u_i, v_j \rangle = 0$. Similarly, we have $\mathbb{U}_y, \mathbb{V}_y, \mathbb{E}_y$ refer to user, item, and interaction set for the domain Y , respectively. Given $\mathbb{E}_x, \mathbb{E}_y$ as training data, and new query users *with no* interactions observed on the target domain, our objective is to predict the next item of interaction. We

¹This simplified Gaussian example is used for illustration purpose.

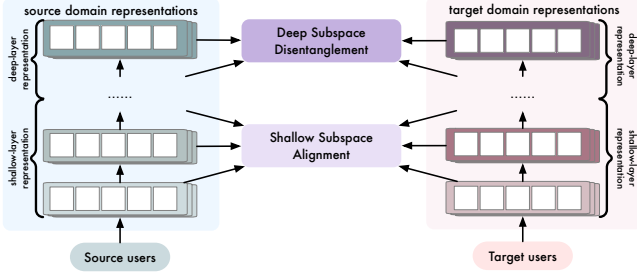


Figure 2: Overview of HJID. Following the FH principle, it separates the user representations into shallow and deep subspaces corresponding to the neural encoder layers. The shallow subspace encodes general features, enforced to be aligned between domains; while the deep subspace parameterizes more domain-oriented factors which are further disentangled into stable domain-shared and variant domain-specific facet, identified by a causal discovery structure.

study a bi-directional CDR setting following [10, 13], where either X or Y can serve as the source domain for predictions in the other.

To facilitate this CDR prediction, we ensure the identifiability of the joint distribution over user representations across domains.

Definition 2.1 (Joint Identifiability). Consider the set of latent factors \mathcal{Z} and the mapping function $f : \mathcal{Z} \rightarrow P(\mathbf{U}_x, \mathbf{U}_y | \mathcal{Z})$, with joint distribution $P(\mathbf{U}_x, \mathbf{U}_y | \mathcal{Z})$ denotes the cross-domain user representation. *Joint identifiability* in contexts of CDR is achieved if and only if f is injective,

$$\mathbf{Z}_1 \neq \mathbf{Z}_2 \iff P(\mathbf{U}_x, \mathbf{U}_y | \mathbf{Z}_1) \neq P(\mathbf{U}_x, \mathbf{U}_y | \mathbf{Z}_2). \quad (1)$$

$\mathbf{Z} \in \mathcal{Z}$ uniquely determines a joint distribution, establishing *joint identifiability* across domains X and Y .

Definition 2.2 (Marginal Identifiability). In the CDR context, *joint identifiability* is relaxed to *marginal identifiability* if, there exist both marginal distributions $P(\mathbf{U}_x | \mathbf{Z}_1)$ and $P(\mathbf{U}_y | \mathbf{Z}_2)$, individually determined by latent factors $\mathbf{Z}_1, \mathbf{Z}_2 \in \mathcal{Z}$. For mapping function $f : \mathcal{Z} \rightarrow P(\mathbf{U}_x | \mathcal{Z})$ and $f : \mathcal{Z} \rightarrow P(\mathbf{U}_y | \mathcal{Z})$, such that

$$\mathbf{Z}_1 \neq \mathbf{Z}_2 \iff P(\mathbf{U}_x | \mathbf{Z}_1) \neq P(\mathbf{U}_x | \mathbf{Z}_2) \iff P(\mathbf{U}_y | \mathbf{Z}_1) \neq P(\mathbf{U}_y | \mathbf{Z}_2) \quad (2)$$

establishes the marginal identifiability within each domain. In relation to *joint identifiability*, *marginal identifiability* does not ensure the latent factor uniqueness across the cross-domain joint space.

3 METHODOLOGY

Fig. (2) conceptually overviews the proposed HJID. We begin by generating user and item representations for both domains using stacked Graph Neural Network layers [9]. Following the FH principle, we decompose user representations into two subspaces, characterized by shallow-layer and deep-layer representations. For the former, we employ Maximum Mean Discrepancy (MMD) that aligns the low-level, generic representations across domains and enforces *Shallow Subspace Alignment*. For the latter, we introduce *Deep Subspace Disentanglement* anchored in the MC principle, to disentangle the behavioral commonality and variations of user representations across domains. To achieve such disentanglement, we build a causal data generation graph that identifies the cross-domain shared latent

factors from cross-domain variant ones based on *identifiability* of the cross-domain joint distribution. In an effort to characterize the behavioral variance caused by domain shifts, we further employ a generative Flow model [12] to approximate the transformation of the variant factors between domains, ensuring *joint identifiability* for unique parameter recovery.

3.1 Encoding Representations

Previously, CDR methods often relied on strong cross-domain correlations and the concurrence of both shared and specific information among domains. Yet, their performances degrade as domain correlations weaken. We thus adopt the Feature Hierarchy (FH) principle [33, 48] to initially decouple intertwined user representations.

3.1.1 Stackable Representation. Denote randomly initialized embedding for each user and item by \mathbf{u}_D and \mathbf{v}_D with $D = \{x, y\}$ being the domain identifier. Our model is architecture-agnostic, thus any neural network like MLP [38], CNN [30], GCN [18] can be applicable. To demonstrate, we introduce two K -layer VBGEs [9] to produce the representations of users and items in both domains.

$$\mathbf{U}_D^k \leftarrow \begin{cases} \text{VBGE}_k(\bar{\mathbf{A}}_D, \mathbf{u}_D), & k = 1 \\ \text{VBGE}_k(\bar{\mathbf{A}}_D, \mathbf{U}_D^{k-1}), & k \geq 2 \end{cases} \quad \mathbf{V}_x^D \leftarrow \begin{cases} \text{VBGE}_k(\bar{\mathbf{A}}_D^\top, \mathbf{v}_D), & k = 1 \\ \text{VBGE}_k(\bar{\mathbf{A}}_D^\top, \mathbf{V}_D^{k-1}), & k \geq 2 \end{cases} \quad (3)$$

where $\bar{\mathbf{A}}_D$ is the normalized matrix form of interaction sets \mathbf{E}_D ($D = \{x, y\}$) and $\bar{\mathbf{A}}_D^\top$ is the transpose. Since this is not the focus of this study, we omit the details here and refer interested readers to [9, 13].

3.1.2 Decoupled User Representations. Building upon the FH principle [48], we consider shallow subspace to encode universally shared features and deep subspace focuses on more abstract and domain-oriented features. Our hypothesis posits that the general, domain-irrelevant features are encoded in the initial k layers, whereas the subsequent $K-k$ layers specialize in extracting domain-oriented features. Provided this decoupling, we obtain the users representations \mathbf{U}_x by concatenating the shallow features \mathbf{S}_x with deeper features \mathbf{D}_x ,

$$\mathbf{U}_x = [\mathbf{S}_x \| \mathbf{D}_x], \mathbf{S}_x = [\mathbf{U}_x^1 \| \dots \| \mathbf{U}_x^k], \mathbf{D}_x = [\mathbf{U}_x^{k+1} \| \dots \| \mathbf{U}_x^K] \quad (4)$$

$$\mathbf{U}_y = [\mathbf{S}_y \| \mathbf{D}_y], \mathbf{S}_y = [\mathbf{U}_y^1 \| \dots \| \mathbf{U}_y^k], \mathbf{D}_y = [\mathbf{U}_y^{k+1} \| \dots \| \mathbf{U}_y^K]$$

with $\|$ denotes vector concatenation. Analogously, the same operations are performed for domain Y as well.

3.2 Shallow Subspace Alignment

The shallow layers encode universal features across domains. To align these features in the shared shallow subspace, we adopt MMD [4] for minimizing distributional divergence as in established domain adaptation strategies [33, 34, 46]. Specifically, we randomly sample two sets of shallow layer user representations $\mathbf{G}_x \sim \mathbf{S}_x$ and $\mathbf{G}_y \sim \mathbf{S}_y$, using Gaussian kernel $k(\cdot, \cdot)$ as the distance measure with MMD,

$$k(\mathbf{s}_{x_i}, \mathbf{s}_{y_j}) = \exp\left(-\frac{\|\mathbf{s}_{x_i} - \mathbf{s}_{y_j}\|^2}{2\sigma^2}\right), \quad (5)$$

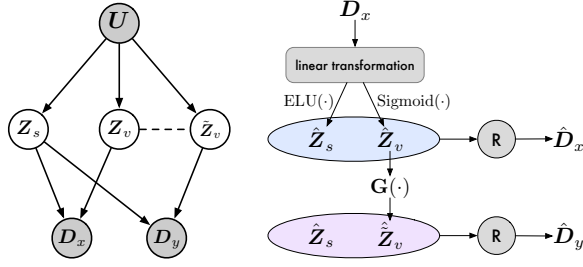


Figure 3: Causal data generation graph (left) and framework (right) of deep subspace disentanglement. The grey circle refers to the observed variables. The dashed line indicates a correlation between two variables. R denotes the reparameterization trick.

where σ is the hyperparameter for the Gaussian kernel. s_{x_i}, s_{y_j} refers to the shallow layer representations of user x_i and user y_j from the sets G_X and G_Y . The computed MMD over all sampled users is

$$\text{MMD}^2(G_X, G_Y) = h \left(\sum_{i=1}^N \sum_{j=1}^N k(s_{x_i}, s_{x_j}) - \sum_{i=1}^N \sum_{j=1}^N k(s_{x_i}, s_{y_j}) + \sum_{i=1}^N \sum_{j=1}^N k(s_{y_i}, s_{y_j}) \right), \quad (6)$$

where $h = \frac{1}{N(N-1)}$ and N is the sample size. Notably, pairwise overlapping among sampled users is not a prerequisite, meaning that the alignment can also be adapted to work with CDR in the absence of overlap users. Minimizing MMD allows us to empirically substantiate the alignment efficacy of general features, ensuring domain consistency at a shallow level.

3.3 Deep Subspace Disentanglement

As aforementioned, we seek a disentanglement of deeper, domain-oriented representations to be domain-shared (stable) and domain-specific (variant) factors, with the former reflecting consistent user behavior and the latter accommodating distribution shifts across domains. In general, it is difficult due to the intertwined effect of complex user behavior [7, 10, 13]. To tackle this, we present the data generation graph for these domain-oriented representations with causality and delve into how to leverage the latent variable model to ensure *joint identifiability*.

3.3.1 Generation Graph for CDR. From a probabilistic perspective, we assume the domain-oriented representations of source domain D_x are generated by latent variables $f: Z \rightarrow D_x$. For disentanglement, the latent variable Z is partitioned into a) the stable portion Z_s and b) variant portion Z_v . The stable portion Z_s characterizes the consistency of the user representation distribution that remains invariant. In contrast, Z_v addresses domain-specific nuances by capturing the observation variances. Similarly, we have $f': Z' \rightarrow D_y$ for the target domain. Z' shares the stable portion with Z_s , while focusing only on the transformations between their variant portions $\tilde{Z}_v = G(Z_v)$. Intuitively, this interprets the observation variance as a result of domain shifts, under the MC principle.

3.3.2 Latent Variable Disentanglement. For simplicity, we model Z as a Gaussian with mean and variance parameterized by Z_s and

Z_v . We first employ non-linear transformations on D_x ,

$$Z \sim \mathcal{N}(Z_s, Z_v) = \mathcal{N}(\text{ELU}(W_s D_x), \text{Sigmoid}(W_v D_x)) \quad (7)$$

where the ELU and the Sigmoid are non-linear activation for Z_s and Z_v , respectively. W_s and W_v are weight parameters, and the bias terms are omitted for brevity.

Note that \tilde{Z}_v can be exclusively transformed from Z_v , without changing Z_s (See Fig. 3). To approximate the mapping $G(\cdot)$, we opt for Normalizing Flow [17, 21, 51] and take advantage of the bijective mappings. Namely, this enables both forward and inverse transformations exact, which facilitates *joint identifiability* of $p(U_x, U_y)$ by ensuring Z_v maps uniquely to \tilde{Z}_v , and vice versa. Consider the marginal distribution $P_X(Z_v)$ and $P_Y(\tilde{Z}_v)$, we can derive the density function of \tilde{Z}_v by

$$P_Y(\tilde{Z}_v) = P_X(f(\tilde{Z}_v)) \det(\text{Df}(\tilde{Z}_v)) = P_X(Z_v) \det(\text{Dg}(Z_v))^{-1} \quad (8)$$

where $f = g^{-1}$ is the inverse of g . $\text{Df}(\cdot) = \frac{\partial f}{\partial \cdot}$ is the Jacobian of f and $\text{Dg}(\cdot) = \frac{\partial g}{\partial \cdot}$ is the Jacobian of g . $\det(\cdot)$ is the matrix determinant. Usually, the limited model expressiveness comes as the downside of bijective transformation. We thus chain a L -layer bijections $G = g_1 \circ \dots \circ g_L$ to improve the model flexibility for when fitting non-linear patterns. Equivalently, Eq.(8) now becomes:

$$P_Y(\tilde{Z}_v) = P_X(G(Z_v)) = P_X(Z_v) \cdot \prod_{l=0}^L \det(\text{Dg}_l(Z_l))^{-1}, \quad (9)$$

with

$$\text{Dg}(Z_v) = \begin{bmatrix} \frac{\partial Z_1}{\partial Z_0} \\ \frac{\partial Z_2}{\partial Z_1} \end{bmatrix} \dots \begin{bmatrix} \frac{\partial Z_v}{\partial Z_{L-1}} \end{bmatrix} = \prod_{l=0}^L \text{Dg}_l(Z_l), \quad (10)$$

The implementation of transformation $\text{Dg}_l(\cdot)$ can be of any choice [12, 20, 37, 39]. We further use the reparameterization trick [26] to sample the domain-oriented representations \hat{D}_x, \hat{D}_y refined by the estimated latent factors \hat{Z}_s, \hat{Z}_v and \tilde{Z}_v ,

$$\hat{D}_x = Z_s + Z_v \odot \epsilon_x, \hat{D}_y = Z_s + \tilde{Z}_v \odot \epsilon_y, \quad (11)$$

with $\epsilon_x \sim N(\mathbf{0}, \mathbf{I})$, $\epsilon_y \sim N(\mathbf{0}, \mathbf{I})$, and $\tilde{Z}_v = G(Z_v)$. \odot denotes element-wise multiplication. We substitute D_x, D_y with \hat{D}_x, \hat{D}_y , leading to refined user representations $\hat{U}_x = [S_x || \hat{D}_x]$ and $\hat{U}_y = [S_y || \hat{D}_y]$.

3.3.3 Marginal vs. Joint Identifiability. We note that what existing methods at most achieve is *marginal identifiability*, as they primarily strive to maximize marginal likelihood $P(U_x)$ or $P(U_y)$, ‘‘averaging out’’ possible influences of other domains. However, this marginalization loses the conditionality between U_x and U_y captured by their joint distribution. Instead, our method leverages Flow-based invertible transformations to ensure that $P(U_x, U_y)$ can be uniquely recovered by Z_v and \tilde{Z}_v jointly.

3.4 Optimization

Having obtained shallow feature consistency and deeper feature disentanglement, we now describe the multi-task objective functions for HJID. Given random groups of users G_X, G_Y , the objectives include 1) MMD that minimizes the divergence between the source and the target shallow representations,

$$\mathcal{L}_s = \text{MMD}^2(G_X, G_Y). \quad (12)$$

2) The deeper subspace disentanglement involves a Flow-based model $G(\cdot)$, which maximizes the predictive likelihood on the target domain after a chain of transformations $G(Z_v)$,

$$\mathcal{L}_G = \sum_{i=1}^N \left[\log p_Y \left(G(Z_v^{(i)}) \right) - \sum_{l=0}^L \log \det \left(Dg_l \left(Z_v^{(i)} \right) \right) \right]. \quad (13)$$

3) To perform accurate CDR predictions, we reconstruct user-item interactions using the inferred latent variables Z . This objective serves dual purposes: stabilizing the optimization of generative model $G(\cdot)$ and enforcing the causal relation between CDR prediction and Z [27]. Moreover, we leverage variational information bottleneck (VIB) [2] to constrain the optimization. Being renowned for excelling at producing informative representations [9, 13], VIB maximizes the mutual information between Z and refined representations \hat{D}_x and \hat{D}_y and removes the redundancy therefrom. [13] shows that the empirical lower bound of VIB can be approximated by the binary cross-entropy loss as

$$\begin{aligned} I((Z_s, Z_v); \hat{D}_x) &\geq \\ &\sum_{(u_i, v_j) \in \mathbb{E}_X} \log \sigma(V_x, \hat{D}_x) + \sum_{(u_i, v_j) \notin \mathbb{E}_X} \log(1 - \sigma(V_x, \hat{D}_x)), \\ I((Z_s, \tilde{Z}_v); \hat{D}_y) &\geq \\ &\sum_{(u_i, v_j) \in \mathbb{E}_Y} \log \sigma(V_y, \hat{D}_y) + \sum_{(u_i, v_j) \notin \mathbb{E}_Y} \log(1 - \sigma(V_y, \hat{D}_y)), \end{aligned} \quad (14)$$

where $\sigma(\cdot)$ is inner product with Sigmoid.

Summing all tasks up yields the overall optimization objective,

$$\mathcal{L} = \mathcal{L}_s + \mathcal{L}_G + I((Z_s, Z_v); \hat{D}_x) + I((Z_s, \tilde{Z}_v); \hat{D}_y). \quad (15)$$

4 EXPERIMENTS

Here are the research questions we aim to answer:

- RQ1) Does HJID outperform existing CDR methods?
- RQ2) If needed, does HJID still demonstrate efficacy even with challenging non-overlap CDR predictions?
- RQ3) Do individual components contribute positively to HJID?
- RQ4) How do hyperparameters impact model performance?

4.1 Experimental setup

4.1.1 Datasets. We conduct all empirical studies on the widely studied Amazon reviews datasets². To showcase the impact of domain correlations, we build 6 pairwise CDR settings: Game-Video and Cloth-Sport are strong-correlation tasks, and Game-Cloth, Game-Sport, Video-cloth, and Video-Game are weak-correlation tasks. All the baselines and our model are evaluated on 6 tasks to evaluate the model performance comprehensively. The detailed information is shown in Table.1.

4.1.2 Compared methods. We introduce eight baselines for comparisons: For **Alignment** methods, we import **CMF** [40] and **LFM** [1]. For **Bridge** methods, we employ **EMCDR** [35], implemented with two variants: **EMCDR-MF** in Matrix Factorization and **EMCDR-NGCF** in Neural Graph Collaborative Filtering[45], and **PTUPCDR** [56]. For the latest **Constraint** baselines, four methods are introduced: **DisenCDR** [9], **UniCDR** [8], **CDRIB** [10], and **DPMCDR** [13].

²<https://cseweb.ucsd.edu/jmcauley/datasets/amazon/links.html>

Table 1: Dataset statistics.

No.	Domain	user	#Overlap	item	interactions	Testing	validation
Task 1	Game	25,025	2,179	12,319	157,721	443	434
	Video	19,457		8,751	158,984		
Task 2	Cloth	41,829	9,828	17,943	194,121	1,972	1,964
	Sport	27,328		12,655	170,426		
Task 3	Game	17,299	5,968	9,125	104,034	1,200	1,192
	Cloth	57,929		25,196	297,241		
Task 4	Game	19,465	3,442	9,834	116,914	690	688
	Sport	38,996		16,964	255,959		
Task 5	Video	19,623	2,001	8,989	167,615	401	400
	Cloth	70,183		31,282	388,224		
Task 6	Video	19,648	2,159	8,781	164,457	439	430
	Sport	41,939		18,208	278,036		

4.1.3 Implementation details. We divide all overlapped users into training(60%), testing(20%), and validation(20%). All non-overlapped users are only used for training. Following common practice [28] as with most studies, we evaluate our model and comparison methods using *leave-one-out* method: only 1 positive item and 999 random-selected negative items are calculated. We report 3 evaluation metrics of predictive performance: Mean Reciprocal Rank (MRR), Hit Rate (HR@{10, 20, 30}), and Normalized Discounted Cumulative Gain (NDCG@{10, 20, 30}). The implementations of **CMF**, **LFM**, **EMCDR**, **PTUPCDR**, **DisenCDR**, **UniCDR**, and **CDRIB** follow the open-sourced codebases, implemented with PyTorch. We implement **DPMCDR** upon CDRIB and make modifications according to [13]. The following are the default settings. The number of VBGE layers K is set to 3. We set the number of shallow layers k to 2. That is, shallow representations and deeper representations become $S_x = [U_x^1 \| U_x^2]$ and $D_x = [U_x^3]$, ($S_y = [U_y^1 \| U_y^2]$ and $D_y = [U_y^3]$ for the target domain). We choose ELU as activation for Z_s for its smooth saturation than the standard ReLU [16] and Sigmoid activation for Z_v since its sensitivity to different distributions [49]. We search embedding size d in the range of {8, 16, 32, 64, 128}. The size of user group N is searched within {16, 32, 64, 128, 256, 512, 1024}. To determine how specific Flows affect the performance, we include 4 transformations MAF[37], NAF[20], NODE[12], and NCSF[39], according to the open-sourced code³. Length of the invertible bijection chain L is searched over {1, 2, 3, 4, 5}. We also investigate the influence of different shallow depths $k=\{1, 2, 3, 4\}$. We use Adam for model optimization.

4.2 Overall performance (RQ1)

As shown in Table. 2, we report the average results (with std) of all CDR tasks over six independent runs. The best results are **bolded**, and the second-runnerup results are underlined. Generally speaking, HJID consistently outperforms the state-of-the-art (SOTA) on all CDR scenarios with significant improvements. We discuss our model against each of **Alignment**, **Bridge**, and **Constraint** methods below.

4.2.1 Comparison with Alignment methods. CMF directly shares representations of overlapping users in both domains without considering shared and unique information within each domain. Unfortunately, this leads to unreliable results in both domains. In contrast, LFM models the user's different representations with a latent variable, allowing for certain user-specificity across domains. While LFM outperforms CMF in most evaluation metrics, these Alignment methods falter owing to the inability to separate domain-shared from domain-specific features. Meanwhile, they face challenges

³<https://github.com/francois-rozet/zuko>

Table 2: Overall performance(%). Improved shows the improvement over the runner-up results. * indicates that the improvement is statistically significant when the HJID and the best baseline are compared with a paired t-test level of $p < 0.05$.

Methods	Game							Video						
	MRR	NDCG@10	NDCG@20	NDCG@30	HR@10	HR@20	HR@30	MRR	NDCG@10	NDCG@20	NDCG@30	HR@10	HR@20	HR@30
CMF	0.91(±0.08)	0.41(±0.15)	0.61(±0.10)	1.05(±0.08)	1.04(±0.31)	1.82(±0.32)	3.91(±0.55)	0.84(±0.07)	0.45(±0.08)	0.82(±0.08)	0.98(±0.08)	1.30(±0.10)	2.86(±0.14)	3.65(±0.80)
LFM	1.68(±0.13)	1.18(±0.13)	1.54(±0.10)	1.9(±0.12)	2.44(±0.16)	3.84(±0.16)	5.6(±0.37)	1.86(±0.24)	1.36(±0.22)	1.82(±0.23)	2.14(±0.23)	2.76(±0.25)	4.56(±0.27)	6.08(±0.29)
EMCDR-MF	1.46(±0.37)	0.89(±0.35)	1.46(±0.36)	1.80(±0.41)	1.56(±0.55)	3.91(±0.55)	5.47(±0.55)	0.98(±0.55)	0.64(±0.13)	0.97(±0.07)	1.25(±0.39)	1.82(±0.38)	3.13(±0.32)	4.43(±0.39)
EMCDR-NGCF	1.51(±0.08)	1.07(±0.23)	1.65(±0.10)	2.26(±0.34)	2.34(±1.10)	4.69(±0.55)	7.55(±1.69)	1.11(±0.11)	0.70(±0.27)	0.98(±0.46)	1.14(±0.36)	1.56(±0.84)	2.86(±0.66)	3.65(±0.85)
PTUPCDR	1.76(±0.45)	1.23(±0.69)	2.00(±0.55)	2.61(±0.43)	2.34(±1.46)	5.47(±0.96)	8.33(±0.32)	1.39(±0.28)	0.89(±0.19)	1.34(±0.39)	1.72(±0.27)	1.56(±0.46)	3.39(±0.59)	5.73(±0.76)
DisenCDR	2.15(±0.10)	1.52(±0.21)	2.32(±0.22)	3.31(±0.37)	3.20(±0.60)	6.41(±0.81)	11.06(±1.41)	2.26(±0.31)	1.59(±0.41)	2.81(±0.52)	3.79(±0.54)	3.57(±0.89)	8.43(±1.40)	13.02(±1.45)
UniCDR	3.02(±0.10)	2.93(±0.21)	3.74(±0.22)	4.21(±0.34)	5.05(±0.70)	8.63(±0.47)	11.18(±0.74)	2.51(±0.38)	2.56(±0.30)	3.23(±0.26)	3.81(±0.28)	5.14(±0.44)	7.80(±0.62)	10.51(±0.72)
CDRIB	4.01(±0.23)	4.52(±0.27)	5.80(±0.35)	6.65(±0.28)	9.32(±0.41)	14.65(±0.74)	18.64(±0.38)	3.78(±0.46)	3.84(±0.51)	5.22(±0.51)	6.12(±0.64)	7.60(±0.74)	13.09(±0.73)	17.34(±1.36)
DPMCDR	4.45(±0.36)	4.80(±0.41)	6.27(±0.28)	7.14(±0.36)	9.51(±0.67)	15.22(±0.57)	19.31(±0.72)	3.67(±0.14)	3.83(±0.14)	5.06(±0.30)	5.96(±0.30)	7.89(±0.32)	12.80(±0.93)	17.00(±1.00)
HJID*	4.63(±0.10)*	4.97(±0.06)*	6.57(±0.10)*	7.43(±0.11)*	9.61(±0.21)*	16.07(±0.20)*	20.11(±0.17)*	4.39(±0.21)*	4.67(±0.19)*	6.00(±0.12)*	6.95(±0.22)*	9.16(±0.15)*	14.48(±0.22)*	18.95(±0.41)*
Improved	3.92%	3.57%	4.84%	4.12%	1.00%	5.63%	4.19%	16.08%	21.45%	14.94%	13.57%	16.05%	10.62%	9.32%
Methods	Cloth							Sport						
	MRR	NDCG@10	NDCG@20	NDCG@30	HR@10	HR@20	HR@30	MRR	NDCG@10	NDCG@20	NDCG@30	HR@10	HR@20	HR@30
CMF	1.42(±0.17)	1.06(±0.15)	1.73(±0.10)	2.00(±0.21)	2.60(±0.43)	4.95(±0.64)	6.25(±0.32)	1.29(±0.12)	1.00(±0.30)	1.59(±0.23)	1.86(±0.12)	2.60(±0.96)	4.95(±0.64)	6.25(±0.32)
LFM	1.48(±0.02)	1.02(±0.06)	1.46(±0.04)	1.84(±0.03)	2.42(±0.10)	4.16(±0.13)	6.94(±0.21)	1.56(±0.22)	1.06(±0.23)	1.52(±0.24)	1.96(±0.22)	2.44(±0.31)	4.32(±0.38)	6.40(±0.33)
EMCDR-MF	1.55(±0.69)	1.27(±0.11)	1.40(±0.04)	2.08(±0.11)	2.60(±0.32)	4.17(±0.32)	5.9(±0.91)	2.04(±0.46)	1.49(±0.46)	1.94(±0.38)	2.22(±0.44)	2.08(±0.32)	4.17(±0.31)	5.21(±0.32)
EMCDR-NGCF	1.98(±0.69)	1.64(±0.85)	1.98(±0.70)	2.37(±0.42)	2.34(±0.96)	3.65(±0.32)	5.47(±0.96)	2.39(±0.68)	1.92(±0.73)	2.50(±0.72)	2.90(±0.86)	3.13(±0.96)	5.47(±0.96)	7.29(±1.59)
PTUPCDR	2.09(±0.30)	2.15(±0.21)	2.47(±0.35)	2.53(±0.41)	3.47(±0.32)	3.65(±0.64)	6.77(±0.96)	1.14(±0.31)	0.55(±0.29)	0.89(±0.52)	1.89(±0.65)	1.56(±0.32)	2.86(±1.28)	7.55(±1.91)
DisenCDR	2.13(±0.12)	1.42(±0.03)	2.29(±0.23)	3.11(±0.52)	3.08(±0.13)	6.58(±0.78)	10.44(±1.14)	2.58(±0.18)	1.54(±0.08)	2.51(±0.12)	3.58(±0.08)	3.22(±0.07)	7.09(±0.27)	12.14(±0.65)
UniCDR	2.70(±0.18)	2.70(±0.23)	3.48(±0.29)	4.03(±0.31)	5.20(±0.48)	8.31(±0.74)	10.93(±0.83)	1.70(±0.15)	1.55(±0.20)	2.11(±0.23)	2.51(±0.25)	3.09(±0.46)	5.33(±0.50)	7.20(±0.57)
CDRIB	3.24(±0.16)	3.40(±0.16)	4.39(±0.13)	5.14(±0.17)	6.54(±0.24)	10.80(±0.17)	14.35(±0.24)	4.17(±0.13)	4.44(±0.12)	5.75(±0.17)	6.61(±0.16)	8.68(±0.25)	13.91(±0.31)	17.95(±0.33)
DPMCDR	2.86(±0.02)	2.88(±0.04)	3.97(±0.05)	4.79(±0.12)	6.00(±0.23)	11.03(±0.12)	14.19(±0.27)	4.12(±0.27)	4.27(±0.27)	5.54(±0.37)	6.46(±0.29)	8.19(±0.34)	13.27(±0.48)	17.63(±0.37)
HJID*	3.43(±0.24)*	3.50(±0.30)*	4.53(±0.31)*	5.31(±0.28)*	6.79(±0.47)*	11.90(±0.53)*	14.54(±0.39)*	4.61(±0.04)*	4.85(±0.08)*	6.26(±0.06)*	7.15(±0.07)*	9.17(±0.30)*	14.77(±0.16)*	19.08(±0.23)*
Improved	5.73%	3.15%	3.26%	3.16%	3.79%	10.18%	1.33%	10.39%	9.24%	8.79%	8.31%	5.53%	6.18%	6.28%
Methods	Game							Cloth						
	MRR	NDCG@10	NDCG@20	NDCG@30	HR@10	HR@20	HR@30	MRR	NDCG@10	NDCG@20	NDCG@30	HR@10	HR@20	HR@30
CMF	1.02(±0.07)	0.74(±0.07)	1.05(±0.09)	1.22(±0.15)	2.08(±0.10)	3.39(±0.16)	4.17(±0.47)	0.98(±0.34)	0.49(±0.02)	0.96(±0.04)	1.28(±0.09)	1.30(±0.13)	3.13(±0.19)	4.95(±0.18)
LFM	1.60(±0.04)	1.06(±0.06)	1.52(±0.07)	1.96(±0.09)	2.28(±0.17)	4.20(±0.20)	6.28(±0.40)	1.62(±0.04)	1.10(±0.17)	1.58(±0.17)	2.00(±0.15)	2.40(±0.13)	4.34(±0.14)	6.30(±0.50)
EMCDR-MF	1.11(±0.06)	0.69(±0.06)	1.02(±0.18)	1.41(±0.19)	2.08(±0.32)	2.86(±0.48)	4.69(±0.84)	1.02(±0.13)	0.48(±0.06)	1.01(±0.24)	1.45(±0.13)	1.30(±0.06)	3.39(±0.05)	6.51(±0.32)
EMCDR-NGCF	1.22(±0.08)	0.91(±0.04)	1.35(±0.12)	1.58(±0.19)	2.86(±0.64)	4.43(±0.32)	5.73(±0.64)	1.06(±0.09)	0.46(±0.25)	1.02(±0.08)	1.52(±0.09)	1.30(±0.16)	4.17(±0.32)	5.73(±0.28)
PTUPCDR	1.57(±0.04)	1.19(±0.02)	1.45(±0.07)	2.74(±0.19)	3.39(±0.67)	3.29(±0.96)	7.29(±0.96)	2.03(±0.21)	1.55(±0.23)	2.21(±0.34)	3.15(±0.13)	2.86(±0.32)	5.47(±0.92)	9.90(±0.36)
DisenCDR	2.15(±0.02)	1.47(±0.16)	2.31(±0.09)	3.04(±0.35)	3.23(±0.34)	6.61(±0.37)	10.07(±1.27)	3.20(±0.54)	2.82(±0.27)	3.44(±0.17)	4.03(±0.69)	4.95(±0.84)	7.40(±0.46)	10.22(±0.70)
UniCDR	2.14(±0.12)	2.10(±0.19)	2.79(±0.21)	3.18(±0.25)	4.16(±0.50)	6.92(±0.71)	8.79(±0.77)	2.28(±0.11)	2.23(±0.12)	2.95(±0.17)	3.49(±0.22)	4.39(±0.25)	7.28(±0.44)	9.80(±0.71)
CDRIB	3.30(±0.08)	3.40(±0.07)	4.43(±0.10)	5.15(±0.08)	6.71(±0.08)	10.83(±0.18)	14.18(±0.09)	3.58(±0.07)	3.63(±0.08)	4.70(±0.09)	5.48(±0.13)	6.86(±0.12)	11.10(±0.18)	14.79(±0.42)
DPMCDR	3.89(±0.19)	4.06(±0.24)	5.26(±0.28)	6.00(±0.27)	7.76(±0.44)	12.54(±0.60)	15.94(±0.59)	3.61(±0.10)	3.72(±0.13)	4.82(±0.09)	5.56(±0.10)	7.19(±0.27)	11.59(±0.08)	15.05(±0.13)
HJID*	4.10(±0.06)*	4.48(±0.04)*	5.55(±0.05)*	6.28(±0.05)*	8.76(±0.07)*	13.04(±0.18)*	16.45(±0.15)*	3.81(±0.05)*	4.00(±0.09)*	5.14(±0.05)*	5.83(±0.08)*	7.72(±0.20)*	12.27(±0.12)*	16.52(±0.23)*
Improved	5.31%	10.44%	5.63%	4.61%	12.92%	4.00%	3.15%	5.66%	7.45%	6.59%	8.79%	7.26%	5.92%	9.74%
Methods	Game							Sport						
	MRR	NDCG@10	NDCG@20	NDCG@30	HR@10	HR@20	HR@30	MRR	NDCG@10	NDCG@20	NDCG@30	HR@10	HR@20	HR@30
CMF	1.45(±0.28)	1.60(±0.13)	2.12(±0.19)	2.56(±0.23)	4.13(±0.61)	5.88(±0.72)	8.29(±0.84)	1.52(±0.21)	1.17(±0.26)	1.43(±0.42)	1.76(±0.37)	2.49(±0.14)	4.21(±0.19)	5.43(±0.85)
LFM	1.48(±0.05)	1.02(±0.04)	1.46(±0.16)	1.84(±0.12)	2.42(±0.15)	4.16(±0.25)	5.94(±0.33)	1.56(±0.11)	1.06(±0.14)	1.52(±0.24)	1.96(±0.28)	2.44(±0.24)	4.32(±0.27)	6.40(±0.54)
EMCDR-MF	1.58(±0.35)	1.60(±0.13)	2.12(±0.19)	2.12(±0.54)	3.34(±0.15)	5.09(±0.19)	5.99(±0.23)	1.39(±0.25)	1.44(±0.21)	1.89(±0.47)	2.50(±0.52)	3.01(±0.32)	5.83(±0.28)	7.36(±0.71)
EMCDR-NGCF	1.35(±0.27)	0.97(±0.33)	1.62(±0.50)	2.12(±0.54)	2.68(±0.28)	7.95(±0.66)	8.63(±0.54)	1.86(±0.06)	1.15(±0.09)	1.66(±0.29)	2.11(±0.36)	2.86(±0.14)	4.95(±0.08)	7.36(±0.27)
PTUPCDR	1.54(±0.30)	1.35(±0.14)	2.05(±0.06)	2.27(±0.08)	2.42(±0.09)	5.02(±0.55)	6.92(±0.14)	1.56(±0.23)	1.33(±0.14)	2.45(±0.20)	2.78(±0.02)	2.90(±0.18)	7.02(±0.37)	8.94(±0.50)
DisenCDR	2.18(±0.08)	1.50(±0.03)	2.80(±0.38)	3.63(±0.57)	3.32(±0.19)	8.52(±1.59)	12.42(±1.43)	2.33(±0.21)	1.72(±0.22)	2.82(±0.39)	3.69(±0.48)	3.87(±0.60)	8.28(±1.28)	12.40(±1.72)
UniCDR	2.65(±0.11)	2.62(±0.08)	3.35(±0.06)	3.92(±0.10)	4.95(±0.03)	7.87(±0.46)	10.56(±0.51)	2.60(±0.42)	2.59(±0.50)	3.38(±0.58)	3.83(±0.60)	4.94(±0.85)	8.07(±1.16)	10.21(±1.24)
CDRIB	3.64(±0.10)	3.88(±0.10)	4.97(±0.11)	5.71(±0.09)	7.71(±0.08)	12.04(±0.15)	15.52(±0.15)	4.25(±0.29)	4.50(±0.29)	5.83(±0.36)	6.64(±0.44)	8.67(±0.42)	13.95(±0.72)	17.76(±1.07)
DPMCDR	3.43(±0.09)	3.61(±0.12)	4.82(±0.08)	5.58(±0.08)	7.28(±0.24)	12.07(±0.24)	15.67(±0.38)	4.01(±0.22)	4.22(±0.38)	5.56(±0.25)	6.39(±0.21)	8.36(±0.43)	13.69(±0.31)	17.63(±0.16)
HJID*	3.92(±0.06)*	4.17(±0.09)*	5.23(±0.06)*	5.97(±0.09)*	7.96(±0.18)*	12.22(±0.07)*	15.70(±0.26)*	4.60(±0.10)*	4.91(±0.10)*	6.32(±0.08)*	7.20(±0.07)*	9.45(±0.21)*	15.05(±0.08)*	19.22(±0.19)*
Improved	7.81%	7.31%	5.33%	4.63%	3.21%	1.52%	1.12%	8.04%	8.98%	8.36%	8.52%	8.94%	7.93%	8.23%
Methods	Video							Cloth						
	MRR	NDCG@10	NDCG@20	NDCG@30	HR@10	HR@20	HR@30	MRR	NDCG@10	NDCG@20	NDCG@30	HR@10	HR@20	HR@30
CMF	1.01(±0.04)	0.45(±0.14)	0.70(±0.09)	1.20(±0.11)	1.04(±0.32)	2.08(±0.64)	4.43(±0.84)	1.20(±0.13)	0.73(±0.07)	1.45(±0.20)	1.89(±0.14)	1.82(±0.32)	4.69(±0.55)	6.77(±0.32)
LFM	1.55(±0.08)	1.07(±0.08)	1.53(±0.17)	1.93(±0.13)	2.54(±0.21)	4.37(±0.31)	6.23(±0.30)	1.64(±0.12)	1.11(±0.13)	1.59(±0.15)	2.06(±0.25)	2.56(±0.16)	4.536(±0.27)	6.72(±0.46)
EMCDR-MF	0.87(±0.49)	0.49(±0.14)	0.80(±0.09)	1.19(±0.49)	1.56(±0.32)	2.86(±0.55)	4.69(±0.32)	1.01(±0.09)	0.70(±0.07)	1.03				

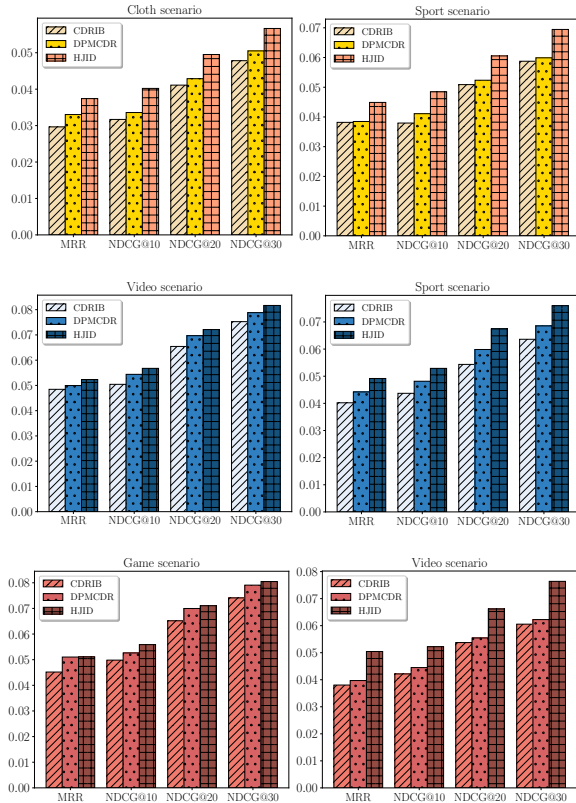


Figure 4: Non-overlapped CDR comparison.

demonstrates the significance of identifying transferable facet from non-transferable factors in comparison with these Bridge methods.

4.2.3 Comparison with Constraint methods. Empirical evidence decisively favors Constraint methods over Alignment and Bridge counterparts, highlighting the utility of optimization constraints in aligning domain-shared attributes. As an example, DPMCDR, the best performer among the Constraint family, significantly leads PTUPCDR by 4.53% and 4.24% in terms of NDCG@30 for the Game-Video CDR task. However, these methods have yet to demonstrate consistent robustness across all CDR tasks, especially when domains are weakly correlated, such as Game-Sport. In particular, DisenCDR experiences performance variances of 1.43% and 1.72% with HR@30. To address this, CDRIB and DPMCDR employ VIB to constrain the user/item representations that effectively concentrate on domain-shared information. Nevertheless, none of these methods have paid sufficient attention to the remaining attributes, i.e., the domain-specific factors grounded in user representations. In contrast, HJID seeks to address both stable, domain-shared and variant, domain-specific factors with a causally-informed disentanglement. As a result, HJID demonstrates the best performances among all CDR tasks, regardless of their correlations.

4.3 Non-overlapped CDR scenario (RQ2)

Non-overlap CDR is an extremely challenging setting, where the model has to successfully extract the common yet adaptable user pattern from observations and make predictions when the training data have no overlapped users between domains. To answer RQ2,

Table 3: Ablation study

Methods	Game			Video		
	MRR	NDCG@30	HR@30	MRR	NDCG@30	HR@30
A	0.0478	0.0720	0.1840	0.0426	0.0648	0.1704
B	0.0357	0.0620	0.1783	0.0387	0.0604	0.1640
C	0.0488	0.0753	0.2011	0.0393	0.0635	0.1803
D	0.0452	0.0683	0.1755	0.0418	0.0677	0.1856
HJID	0.0474	0.0766	0.2026	0.0467	0.0730	0.1958

Methods	Game			Cloth		
	MRR	NDCG@30	HR@30	MRR	NDCG@30	HR@30
A	0.0376	0.0586	0.1545	0.0369	0.0556	0.1460
B	0.0362	0.0566	0.1526	0.0350	0.0533	0.1407
C	0.0363	0.0576	0.1561	0.0359	0.0536	0.1401
D	0.0381	0.0591	0.1590	0.0355	0.0547	0.1472
HJID	0.0420	0.0635	0.1645	0.0376	0.0579	0.1651

Methods	Cloth			Sport		
	MRR	NDCG@30	HR@30	MRR	NDCG@30	HR@30
A	0.0351	0.0553	0.1504	0.0408	0.0644	0.1755
B	0.0289	0.0485	0.1442	0.0275	0.0404	0.1045
C	0.0281	0.0452	0.1305	0.0441	0.0671	0.1720
D	0.0344	0.0521	0.1372	0.0420	0.0675	0.1849
HJID	0.0383	0.0577	0.1583	0.0458	0.0708	0.1902

we modify the training dataset to contain only non-overlapped users, and keep the same set of overlapped users, as in the overlapped CDR scenario, for testing and validation. Due to the page limitation, we compare HJID with CDRIB and DPMCDR, the top-2 performers among all baselines, for three CDR settings.

Fig. 4 illustrates that DPMCDR outperforms CDRIB in all metrics. Similar to HJID, DPMCDR dispenses with the necessity for exact user overlap as anchors. Conversely, CDRIB still relies on overlapped users for building cross-domain correspondence. As the optimization operates over the distributional level, HJID also sidesteps the pairwise correspondence of overlap users, opting instead to enforce causal *joint identifiability* to capture cross-domain correlations. Thanks to the latent disentanglement and *joint identifiability*, HJID is able to model both behavioral invariance and variance under domain shifts.

4.4 Ablation Studies (RQ3)

To address RQ3, we systematically evaluate the impact of several model variants by removing partial components from the full HJID. Variant A removes G and performs representation encoding only; Variant B aligns representations in both shallow and deep subspace simultaneously, without identifying non-transferable factors; Variant C removes the invertible Flow-based transformations $G(\cdot)$; Variant D abandons the feature hierarchy principle and applies representation disentanglement for the whole encoder neural network. Here we report the results with Game-Video, Cloth-Sport, and Game-Cloth in Table. 3 due to page limitation.

Concretely, variant A can be seen as a baseline without cross-domain adaptation. Variant B can be interpreted as a member of the Alignment family. Variant C solely applies MMD to the shallow layers, and thus can be seen as a typical domain adaptation strategy resembling [33]. As shown in Table. 3, in all three tasks, Variant A outperforms Variant B in terms of all metrics. This may suggest that Alignment methods may be unstable in certain cases, since they inappropriately align non-transferable attributes. In combating the non-transferability issue, Variant C surpasses Variant B in

several key metrics. Specifically, its MRR observes a boost of 1.33% and 0.31% in the strongly correlated Game-Video task but is barely improved, or even drops in the weakly correlated Game-Cloth and cloth-sport tasks, possibly due to scarce shared information and the absence of an identifiable joint user distribution. While Variant D ensures *joint identifiability*, it may overlook that domain-shared information, resulting in varying performance in some cases, such as Game-Video. To sum up, the full HJID consistently outperforms all other variants by establishing causal relationships in user representations and ensuring *identifiable* joint distribution of cross-user representation, regardless of domain correlation strength.

4.5 Parameter sensitivity (RQ 4)

We search the best value of the following parameters: user group size N , the invertible transformation and its chain length L , number of VBGE layers K , the depth of shallow layers k , and embedding size throughout the encoder neural network. The results in 6 CDR tasks are shown in Fig. 5.

A small group size allows the best performance of HJID, with the runner-up results when the group size is large. We first evaluate the impact of **group size** N . All metrics achieve the best performance when group size $N=16$. A smaller group size allows our model to gradually approach the optimal solution through multiple iterations. We also observed a similar performance when the group size is sufficiently large. This could be attributed to the substantial number of random samples, enabling our model to fit the target joint distribution effectively.

HJID shows stable results when NCSF is used to generate variant parts in most tasks. We then compare four **Flow-based models** (MAF, NAF, NODE, NCSF) as the design choice of invertible transformations. In the Game-Sport and Video-Sport tasks, HJID attains the best performance with NCSF, whereas NAF delivers the highest performance in the Video-Cloth and Game-Cloth tasks. For a thorough comparison, we additionally conduct experiments with **varying layers** for both NAF and NCSF. **The experimental results of 2-layer and 3-layer NCSF exhibit substantial similarity.** In the Video-Sport task, 3-layer NAF performs the best, while in the Game-Sport task, 5-layer NCSF excels. This emphasizes the importance of tailoring the model architecture according to the task at hand.

We extend our investigation to determine the optimal number of **VBGE layers** K in $\{2, 3, 4, 5\}$. The single-layer VBGE is not considered, as HJID requires a minimum of two layers for proper implementation. Empirical results indicate that a **3-layer VBGE configuration yields superior performance across multiple metrics**. Subsequently, we fix $K=5$ and examine the **most effective shallow layers** k for shallow subspace alignment within $\{1, 2, 3, 4\}$. The optimal value of k varies among different CDR tasks. **Higher aligned layers possess superior results**, encouraging HJID to decouple user representations into shallow-layer and deep-layer representations at higher levels.

Finally, we assess the **embedding size** d with 3-layer VBGEs and NCSF. Since we concatenate the outputs of each layer, the size of representations spans across $\{24, 48, 128, 192, 384\}$. **Optimal embedding sizes vary across different scenarios.** The metrics exhibit an initial rise followed by a decline, with the optimal performance achieved at $d=64$ for Game-Sport and $d=32$ for Video-Cloth.

5 RELATED WORK

As of today, CDR methods fall into one of three categories: **Alignment** method [1, 14, 15, 40], **Bridge** method [3, 7, 22, 32, 35, 52, 53, 55, 56], and **Constraint** method [8–10, 13].

For the **alignment method**, previous works share representations or align user representations in the latent space. For example, CMF[40] is the first to factorize matrices of different domains simultaneously and directly share the embeddings of shared users across domains. LFM[1] assumes that representations are generated from a user-specific global latent factor. CLFM[15] represents the cluster-level rating patterns of domains into a latent space. Also, MV-DNN[14] constructs a single mapping for user features and leverages information from interactions to a unified latent space.

As for **bridge methods**, their goal is to construct transformation functions across domains with bespoke neural architectures. For example, EMCDR[35] first proposes the embedding-and-mapping approach and applies the Multi-Layer Perception (MLP) as the only transformation bridge to transfer information from the source to the target domain. following, DCDCSR[53], SSCDR[22], DTCDR[52], HCDIR[3], DDTCDR[32], TMCDDR[55], and PTUPCDR[56] obey the same procedure to capture cross-domain correlations between domains. For example, DCDCSR introduces DNN to generate latent factors across domains with the consideration of rating sparsity degrees. HCDIR uses MLP to model the correlations between user representations in the latent space. Moreover, TMCDDR utilizes a meta-network to achieve good generalization in few-shot CDR, while PTUPCDR employs the meta-based network to generate personalized transformation bridges. C^2 DSR maximizes the mutual information between single-domain and cross-domain representations for unbiased information within and across domains.

However, these methods assumed a complete sharing of user representations across domains, ignoring the potential for negative transfer caused by non-transferable features. To address this, recent researchers introduced various **constraints** to enhance the focus on sharable parts within user representations. Specifically, DisenCDR[9] designs regularizers for overlapped and non-overlapped users to distinguish domain-shared and domain-specific information. Similarly, CDRIB[10] incorporates variational information bottleneck into optimization to encourage the model to prioritize domain-shared information. DPMCDR[13] summarizes user preferences as a domain-level preference distribution and aligns the invariant preferences of two domains using JS divergence. Moreover, UniCDR[8] employs contrastive learning with domain masking mechanisms to constrain encoding domain invariant information.

Unlike previous methods that focus overwhelmingly on domain-shared information, our approach challenges their efficacy and disentangles domain-shared and domain-specific representations from the intertwined user representation and models the correlation between domain-specific factors and domain-shared factors in different domains in different domains based on data generation graphs, thus achieving CDR grounded in reasonable causal effect. More importantly, our method ensures predictive robustness by establishing *identifiability* of the joint distribution across domains.

6 CONCLUSION AND FUTURE WORKS

We have presented a causal subspace disentanglement method that resolves issues in identifying cross-domain joint distribution, while

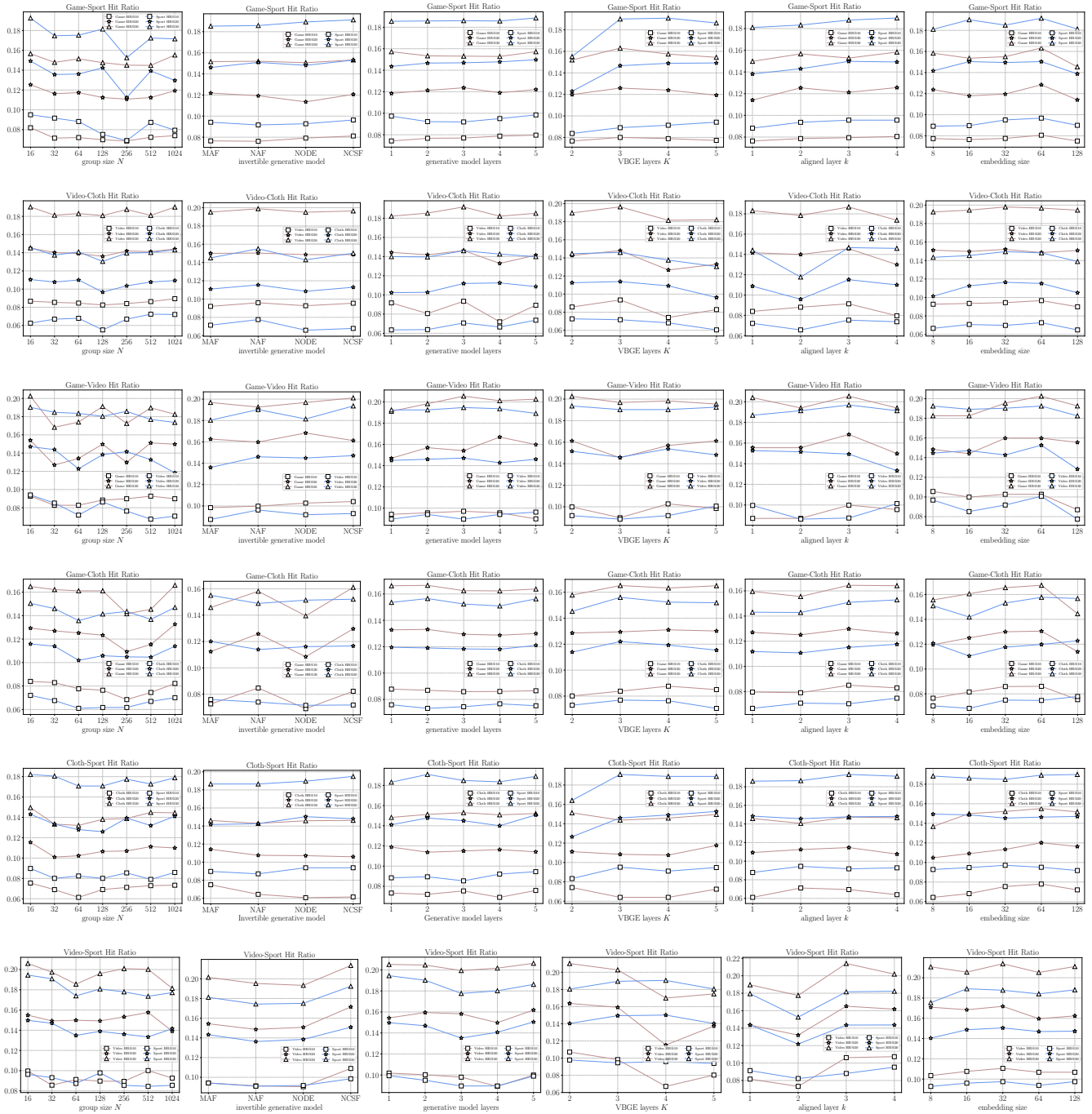


Figure 5: Parameter evaluation in 6 CDR tasks.

maintaining cross-domain consistency and domain-specific properties. Particularly, we divided user representations into shallow general features and deep domain-oriented features, according to the Hierarchical Feature Representation principle. As a way to align domain-irrelevant general features, we employed Maximum Mean Discrepancy to domain-shared representations in shallow subspace. We then ensured the *identifiability* of cross-domain joint

distributions by building a causal data generation graph with disentangled deep-layer latent variables. Empirical assessments in the real world show HJID’s superior performance over existing methods, establishing a new state-of-the-art. Future work will focus on uncovering cross-domain causal relationships and model generalization to multi-domain aligned contexts.

REFERENCES

- [1] Deepak Agarwal, Bee-Chung Chen, and Bo Long. 2011. Localized factor models for multi-context recommendation. In *Proceedings of the 17th ACM SIGKDD international conference on Knowledge discovery and data mining*. 609–617.
- [2] Alexander A Alemi, Ian Fischer, Joshua V Dillon, and Kevin Murphy. 2016. Deep variational information bottleneck. *arXiv preprint arXiv:1612.00410* (2016).
- [3] Ye Bi, Liqiang Song, Mengqiu Yao, Zhenyu Wu, Jianming Wang, and Jing Xiao. 2020. A heterogeneous information network based cross domain insurance recommendation system for cold start users. In *Proceedings of the 43rd international ACM SIGIR conference on research and development in information retrieval*. 2211–2220.
- [4] Karsten M Borgwardt, Arthur Gretton, Malte J Rasch, Hans-Peter Kriegel, Bernhard Schölkopf, and Alex J Smola. 2006. Integrating structured biological data by kernel maximum mean discrepancy. *Bioinformatics* 22, 14 (2006), e49–e57.
- [5] Gerhard Brewka and Joachim Hertzberg. 1993. How to do things with worlds: On formalizing actions and plans. *Journal of Logic and Computation* 3, 5 (1993), 517–532.
- [6] Iván Cantador, Ignacio Fernández-Tobías, Shlomo Berkovsky, and Paolo Cremonesi. 2015. Cross-domain recommender systems. *Recommender systems handbook* (2015), 919–959.
- [7] Jiangxia Cao, Xin Cong, Jiawei Sheng, Tingwen Liu, and Bin Wang. 2022. Contrastive Cross-Domain Sequential Recommendation. In *Proceedings of the 31st ACM International Conference on Information & Knowledge Management*. 138–147.
- [8] Jiangxia Cao, Shaoshuai Li, Bowen Yu, Xiaobo Guo, Tingwen Liu, and Bin Wang. 2023. Towards Universal Cross-Domain Recommendation. In *Proceedings of the Sixteenth ACM International Conference on Web Search and Data Mining*. 78–86.
- [9] Jiangxia Cao, Xixun Lin, Xin Cong, Jing Ya, Tingwen Liu, and Bin Wang. 2022. Disencdr: Learning disentangled representations for cross-domain recommendation. In *Proceedings of the 45th International ACM SIGIR Conference on Research and Development in Information Retrieval*. 267–277.
- [10] Jiangxia Cao, Jiawei Sheng, Xin Cong, Tingwen Liu, and Bin Wang. 2022. Cross-domain recommendation to cold-start users via variational information bottleneck. In *2022 IEEE 38th International Conference on Data Engineering (ICDE)*. IEEE, 2209–2223.
- [11] Hao Chen, Zefan Wang, Feiran Huang, Xiao Huang, Yue Xu, Yishi Lin, Peng He, and Zhoujun Li. 2022. Generative adversarial framework for cold-start item recommendation. In *Proceedings of the 45th International ACM SIGIR Conference on Research and Development in Information Retrieval*. 2565–2571.
- [12] Ricky TQ Chen, Yulia Rubanova, Jesse Bettencourt, and David K Duvenaud. 2018. Neural ordinary differential equations. *Advances in neural information processing systems* 31 (2018).
- [13] Jing Du, Zesheng Ye, Bin Guo, Zhiwen Yu, and Lina Yao. 2023. Distributional Domain-Invariant Preference Matching for Cross-Domain Recommendation. [arXiv:2309.01343 \[cs.LG\]](https://arxiv.org/abs/2309.01343)
- [14] Ali Mamdouh Elkahky, Yang Song, and Xiaodong He. 2015. A multi-view deep learning approach for cross domain user modeling in recommendation systems. In *Proceedings of the 24th international conference on world wide web*. 278–288.
- [15] Sheng Gao, Hao Luo, Da Chen, Shantao Li, Patrick Gallinari, and Jun Guo. 2013. Cross-domain recommendation via cluster-level latent factor model. In *Machine Learning and Knowledge Discovery in Databases: European Conference, ECML PKDD 2013, Prague, Czech Republic, September 23-27, 2013, Proceedings, Part II 13*. Springer, 161–176.
- [16] Bertil Grelsson and Michael Felsberg. 2018. Improved learning in convolutional neural networks with shifted exponential linear units (ShELUs). In *2018 24th International Conference on Pattern Recognition (ICPR)*. IEEE, 517–522.
- [17] Jiayan Guo, Peiyan Zhang, Chaozhuo Li, Xing Xie, Yan Zhang, and Sunghun Kim. 2022. Evolutionary preference learning via graph nested gru ode for session-based recommendation. In *Proceedings of the 31st ACM International Conference on Information & Knowledge Management*. 624–634.
- [18] Will Hamilton, Zhitao Ying, and Jure Leskovec. 2017. Inductive representation learning on large graphs. *Advances in neural information processing systems* 30 (2017).
- [19] Biwei Huang, Kun Zhang, Jiji Zhang, Joseph Ramsey, Ruben Sanchez-Romero, Clark Glymour, and Bernhard Schölkopf. 2020. Causal discovery from heterogeneous/nonstationary data. *The Journal of Machine Learning Research* 21, 1 (2020), 3482–3534.
- [20] Chin-Wei Huang, David Krueger, Alexandre Lacoste, and Aaron Courville. 2018. Neural autoregressive flows. In *International Conference on Machine Learning*. PMLR, 2078–2087.
- [21] Jinsung Jeon, Soyoun Kang, Minju Jo, Seunghyeon Cho, Noseong Park, Seonhoon Kim, and Chiyoun Song. 2021. Lightmove: A lightweight next-poi recommendation for taxicab rooftop advertising. In *Proceedings of the 30th ACM International Conference on Information & Knowledge Management*. 3857–3866.
- [22] SeongKu Kang, Junyoung Hwang, Dongha Lee, and Hwanjo Yu. 2019. Semi-supervised learning for cross-domain recommendation to cold-start users. In *Proceedings of the 28th ACM International Conference on Information and Knowledge Management*. 1563–1572.
- [23] Muhammad Murad Khan, Roliana Ibrahim, and Imran Ghani. 2017. Cross domain recommender systems: a systematic literature review. *ACM Computing Surveys (CSUR)* 50, 3 (2017), 1–34.
- [24] Sangeet Khemlani and PN Johnson-Laird. 2013. Cognitive changes from explanations. *Journal of Cognitive Psychology* 25, 2 (2013), 139–146.
- [25] Sangeet Khemlani and Phil Johnson-Laird. 2015. Domino effects in causal contradictions. In *CogSci*.
- [26] Diederik P Kingma and Max Welling. 2013. Auto-encoding variational bayes. *arXiv preprint arXiv:1312.6114* (2013).
- [27] Lingjing Kong, Shaoan Xie, Weiran Yao, Yujia Zheng, Guangyi Chen, Petar Stojanov, Victor Akinwande, and Kun Zhang. 2022. Partial disentanglement for domain adaptation. In *International Conference on Machine Learning*. PMLR, 11455–11472.
- [28] Walid Krichene and Steffen Rendle. 2020. On sampled metrics for item recommendation. In *Proceedings of the 26th ACM SIGKDD international conference on knowledge discovery & data mining*. 1748–1757.
- [29] Jogendra Nath Kundu, Suvaansh Bhamri, Akshay R Kulkarni, Hiran Sarkar, Varun Jampani, et al. 2022. Subsidiary prototype alignment for universal domain adaptation. *Advances in Neural Information Processing Systems* 35 (2022), 29649–29662.
- [30] Yann LeCun, Léon Bottou, Yoshua Bengio, and Patrick Haffner. 1998. Gradient-based learning applied to document recognition. *Proc. IEEE* 86, 11 (1998), 2278–2324.
- [31] Chenglin Li, Mingjun Zhao, Huanming Zhang, Chenyun Yu, Lei Cheng, Guoqing Shu, BeiBei Kong, and Di Niu. 2022. RecGURU: Adversarial Learning of Generalized User Representations for Cross-Domain Recommendation. In *Proceedings of the Fifteenth ACM International Conference on Web Search and Data Mining (WSDM '22)*. Association for Computing Machinery, 571–581.
- [32] Pan Li and Alexander Tuzhilin. 2020. Ddtdcr: Deep dual transfer cross domain recommendation. In *Proceedings of the 13th International Conference on Web Search and Data Mining*. 331–339.
- [33] Mingsheng Long, Yue Cao, Jianmin Wang, and Michael Jordan. 2015. Learning transferable features with deep adaptation networks. In *International conference on machine learning*. PMLR, 97–105.
- [34] Mingsheng Long, Han Zhu, Jianmin Wang, and Michael I Jordan. 2017. Deep transfer learning with joint adaptation networks. In *International conference on machine learning*. PMLR, 2208–2217.
- [35] Tong Man, Huawei Shen, Xiaolong Jin, and Xueqi Cheng. 2017. Cross-domain recommendation: An embedding and mapping approach. In *IJCAI*, Vol. 17. 2464–2470.
- [36] Maurice Pagnucco and Pavlos Peppas. 2001. Causality and minimal change demystified. In *IJCAI*. 125–130.
- [37] George Papamakarios, Theo Pavlakou, and Iain Murray. 2017. Masked autoregressive flow for density estimation. *Advances in neural information processing systems* 30 (2017).
- [38] Tapani Raiko, Harri Valpola, and Yann LeCun. 2012. Deep learning made easier by linear transformations in perceptrons. In *Artificial intelligence and statistics*. PMLR, 924–932.
- [39] Danilo Jimenez Rezende, George Papamakarios, Sébastien Racanière, Michael Albergo, Gurtje Kanwar, Phiala Shanahan, and Kyle Cranmer. 2020. Normalizing flows on tori and spheres. In *International Conference on Machine Learning*. PMLR, 8083–8092.
- [40] Ajit P Singh and Geoffrey J Gordon. 2008. Relational learning via collective matrix factorization. In *Proceedings of the 14th ACM SIGKDD international conference on Knowledge discovery and data mining*. 650–658.
- [41] Petar Stojanov, Mingming Gong, Jaime Carbonell, and Kun Zhang. 2019. Data-driven approach to multiple-source domain adaptation. In *The 22nd International Conference on Artificial Intelligence and Statistics*. PMLR, 3487–3496.
- [42] Julius Von Kügelgen, Yash Sharma, Luigi Gresele, Wieland Brendel, Bernhard Schölkopf, Michel Besserve, and Francesco Locatello. 2021. Self-supervised learning with data augmentations provably isolates content from style. *Advances in neural information processing systems* 34 (2021), 16451–16467.
- [43] Boyu Wang, Jorge Mendez, Mingbo Cai, and Eric Eaton. 2019. Transfer learning via minimizing the performance gap between domains. *Advances in neural information processing systems* 32 (2019).
- [44] Tianxin Wang, Fuzhen Zhuang, Zhiqiang Zhang, Daixin Wang, Jun Zhou, and Qing He. 2021. Low-dimensional alignment for cross-domain recommendation. In *Proceedings of the 30th ACM International Conference on Information & Knowledge Management*. 3508–3512.
- [45] Xiang Wang, Xiangnan He, Meng Wang, Fuli Feng, and Tat-Seng Chua. 2019. Neural graph collaborative filtering. In *Proceedings of the 42nd international ACM SIGIR conference on Research and development in Information Retrieval*. 165–174.
- [46] Hongliang Yan, Yukang Ding, Peihua Li, Qilong Wang, Yong Xu, and Wangmeng Zuo. 2017. Mind the class weight bias: Weighted maximum mean discrepancy for unsupervised domain adaptation. In *Proceedings of the IEEE conference on computer vision and pattern recognition*. 2272–2281.
- [47] Xu Yu, Qiang Hu, Hui Li, Junwei Du, Jia Gao, and Lijun Sun. 2022. Cross-domain recommendation based on latent factor alignment. *Neural Computing*

- and Applications* (2022), 1–12.
- [48] Matthew D Zeiler and Rob Fergus. 2014. Visualizing and understanding convolutional networks. In *Computer Vision—ECCV 2014: 13th European Conference, Zurich, Switzerland, September 6–12, 2014, Proceedings, Part I 13*. Springer, 818–833.
- [49] Chao Zhang and Philip C Woodland. 2016. DNN speaker adaptation using parameterised sigmoid and ReLU hidden activation functions. In *2016 IEEE International Conference on Acoustics, Speech and Signal Processing (ICASSP)*. IEEE, 5300–5304.
- [50] Kun Zhang, Mingming Gong, Petar Stojanov, Biwei Huang, Qingsong Liu, and Clark Glymour. 2020. Domain adaptation as a problem of inference on graphical models. *Advances in neural information processing systems* 33 (2020), 4965–4976.
- [51] Ting Zhong, Zijing Wen, Fan Zhou, Goce Trajcevski, and Kunpeng Zhang. 2020. Session-based recommendation via flow-based deep generative networks and Bayesian inference. *Neurocomputing* 391 (2020), 129–141.
- [52] Feng Zhu, Chaochao Chen, Yan Wang, Guanfeng Liu, and Xiaolin Zheng. 2019. Dtdcr: A framework for dual-target cross-domain recommendation. In *Proceedings of the 28th ACM International Conference on Information and Knowledge Management*. 1533–1542.
- [53] Feng Zhu, Yan Wang, Chaochao Chen, Guanfeng Liu, Mehmet Orgun, and Jia Wu. 2018. A deep framework for cross-domain and cross-system recommendations. In *Proceedings of the 27th International Joint Conference on Artificial Intelligence*. 3711–3717.
- [54] Feng Zhu, Yan Wang, Chaochao Chen, Jun Zhou, Longfei Li, and Guanfeng Liu. 2021. Cross-domain recommendation: challenges, progress, and prospects. *arXiv preprint arXiv:2103.01696* (2021).
- [55] Yongchun Zhu, Kaikai Ge, Fuzhen Zhuang, Ruobing Xie, Dongbo Xi, Xu Zhang, Leyu Lin, and Qing He. 2021. Transfer-meta framework for cross-domain recommendation to cold-start users. In *Proceedings of the 44th International ACM SIGIR Conference on Research and Development in Information Retrieval*. 1813–1817.
- [56] Yongchun Zhu, Zhenwei Tang, Yudan Liu, Fuzhen Zhuang, Ruobing Xie, Xu Zhang, Leyu Lin, and Qing He. 2022. Personalized transfer of user preferences for cross-domain recommendation. In *Proceedings of the Fifteenth ACM International Conference on Web Search and Data Mining*. 1507–1515.